ELSEVIER

Bioorganic & Medicinal Chemistry Letters

Bioorganic & Medicinal Chemistry Letters Vol. 17, No. 10, 2007

Contents

ARTICLES

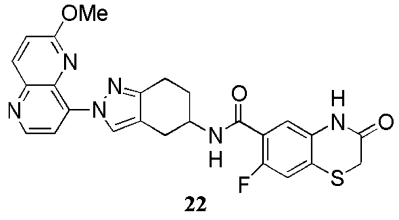

22

DNA Gyrase IC_{50} = 0.12 μg/mL
Topoisomerase IV IC_{50} = 0.125 μg/mL
S. aureus MIC = 0.25 μg/mL

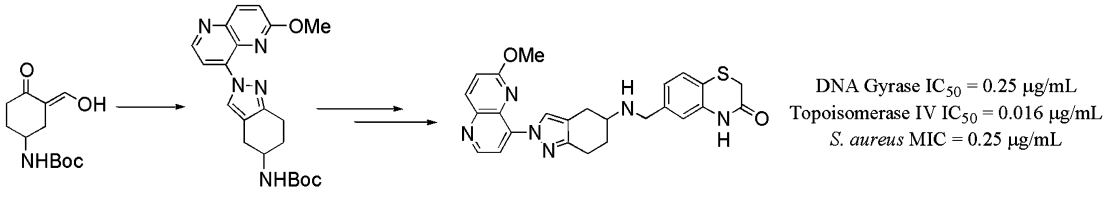

8 13 1a

DNA Gyrase IC_{50} = 0.25 μg/mL
Topoisomerase IV IC_{50} = 0.016 μg/mL
S. aureus MIC = 0.25 μg/mL

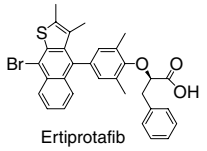

Ertiprotafib

Ertiprotafib was developed as an inhibitor of PTP1B for the treatment of type 2 diabetes, and progressed to a phase II clinical trial. In this study, Ertiprotafib was shown to be a potent inhibitor of IKK-β with an IC_{50} of 400 nM.

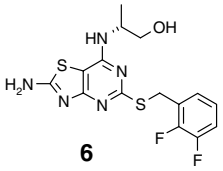

6

The optimisation of antagonists of the CXCR2 receptor is described involving a novel tandem displacement reaction culminating in the synthesis of **6**, a novel, potent and metabolically stable lead compound.

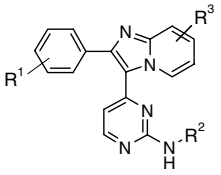

Synthesis of a series of 2-aryl-3-pyrimidyl-imidazo[1,2-*a*]pyridines with potent activity against herpes simplex viruses is described. Synthetic approaches allowing for variation of the 2-aryl, 3-heteroaryl as well as other imidazopyridine substituents are outlined and resulting effects on antiviral activity are highlighted. Several compounds with in vitro antiviral activity similar or better than acyclovir are described.

The biological evaluation of non-covalent FAS II inhibitors containing the imidazopiperidine scaffold against *Mycobacterium tuberculosis* has been carried out with a view to assessment as a potential lead series of compounds. A summary of the chemistry carried out and the evaluation of results is described herein.

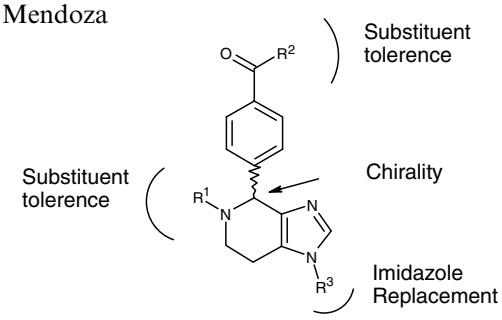

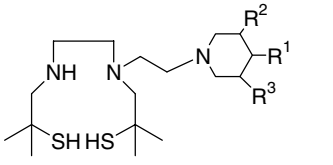

R^1=R^2=R^3=H **NEPDDD**
R^1=CH_3, R^2=R^3=H **NEMPDDD**
R^1=H, R^2=R^3=CH_3 **NEMMPDDD**

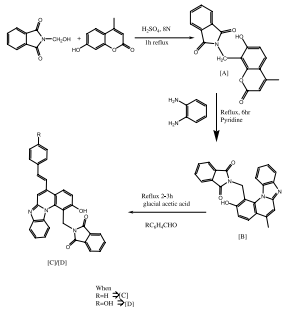

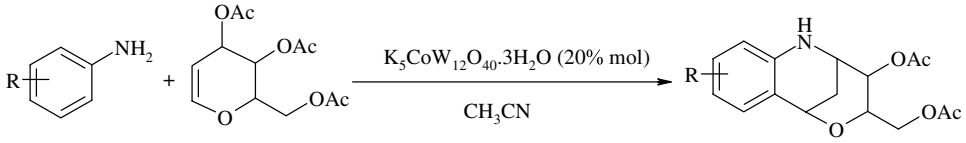

Treatment of 3,4,6-tri-*O*-acetyl-D-glucal with various aryl amines under mild and neutral conditions gave sugar derived tetrahydroquinoline derivates in short reaction times in the presence of $K_5CoW_{12}O_{40}{\cdot}H_2O$ as an environmentally friendly, inexpensive, and reusable catalyst.

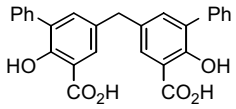

8

Compound **8** inhibited PTP1B in vitro and suppressed diet-induced weight gain in mice.

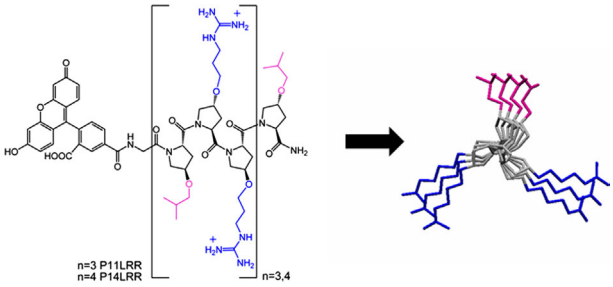

Investigations of length effects and mechanism of cell penetrating peptides displaying a rigid polyproline helix backbone are reported.

We have discovered novel hydantoins, triazolones, and imidazolones that are druglike, non-hydroxamate inhibitors of the Zn-metalloprotease TACE with nM potency. Synthesis, SAR, and MMP selectivity of these inhibitors is described and how they conform to a pharmacophore model of heterocyclic non-hydroxamate TACE inhibitors compared with the IK682-TACE X-ray crystal structure.

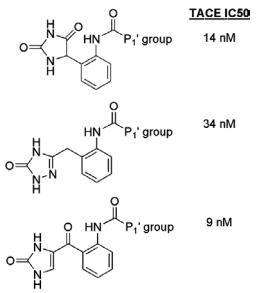

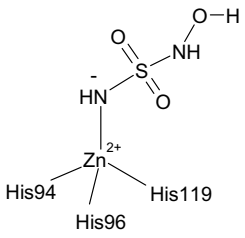

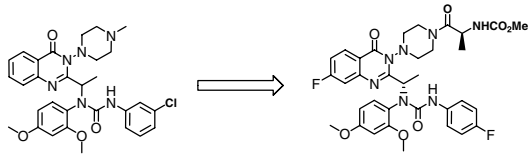

Further structure–activity relationships of a novel series of fungal efflux pump inhibitors with respect to potentiation of the activity of fluconazole against strains of *Candida albicans* and *Candida glabrata* over-expressing ABC-type efflux pumps are systematically explored. Rat protein binding, hepatocyte stability, and pharmacokinetics of selected analogues are reported.

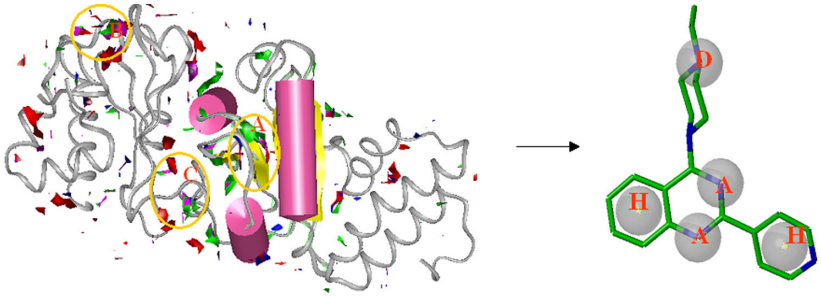

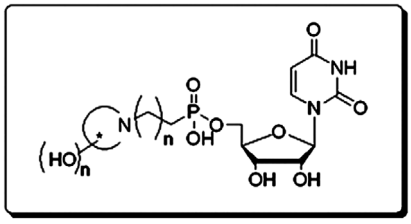

Phosphonoxins, a new class of synthetic, rationally designed anti-microbial agents, are described. From this class a sub-micromolar inhibitor of *Giardia* trophocoite growth has been identified.

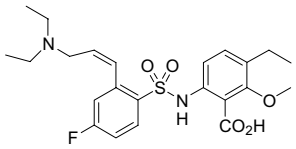

19g: IC_{50}=0.026 μM
EC_{50} (HT-1080)=0.07 μM

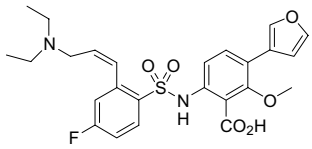

19i: IC_{50}=0.015 μM
EC_{50} (HT-1080)=0.06 μM

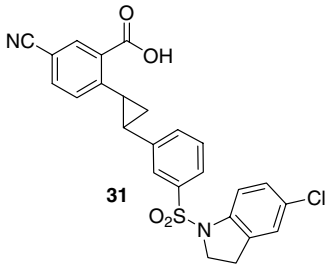

31

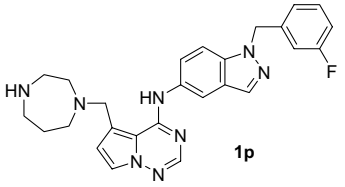

1p

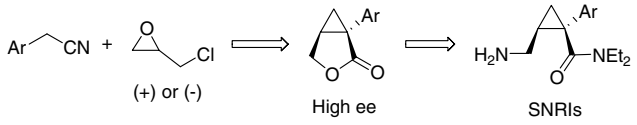

(+) or (-) High ee SNRIs

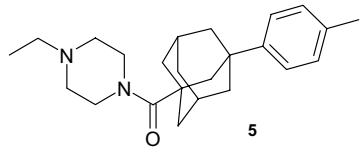

hHSD1 IC_{50} = 82nM

The synthesis and biological activity of a series of adamantyl amide 11β-HSD1 inhibitors represented by **5** is reported.

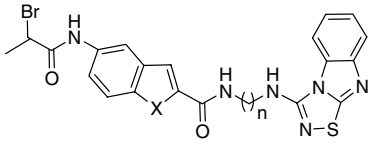

n=3 or 6
X=NH, NCH_3, O or S

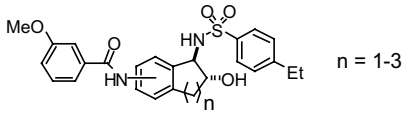

Structure–activity relationship of a new class of Kv1.5 inhibitors based on the indane scaffold was investigated.

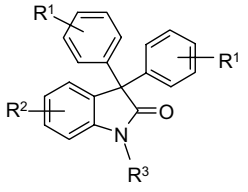

The syntheses and structure–antiproliferative relationship for oxyphenisatin analogues are reported.

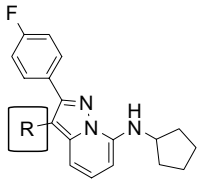

SAR explorations to understand the effects of the C3 substituent on antiviral activity for herpes simplex virus for a series of pyrazolo[1,5-*a*]pyridine derivatives is reported. Resulting data emphasizes the importance of the orientation and basicity of heteroatoms contained in the C3 substituent. During the course of this study, several novel synthetic approaches were developed further elaborating the available synthetic methodology for this important heterocycle.

Bis(indolyl)maleimide pyridinophanes ('multiheterophanes'), from cobalt-mediated [2+2+2] cycloaddition, were found to be potent, selective inhibitors of GSK-3β. An X-ray structure of a co-crystal with GSK-3β is reported.

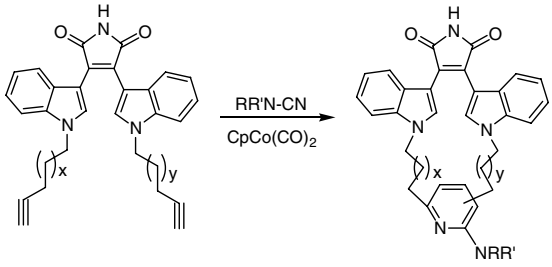

A series of quinoline-based PDE-10A inhibitors was determined to cause insulin secretion in vitro. Optimized compounds were evaluated in vivo where improvements in glucose tolerance and increases in insulin secretion were measured.

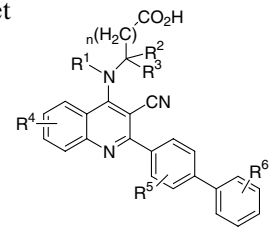

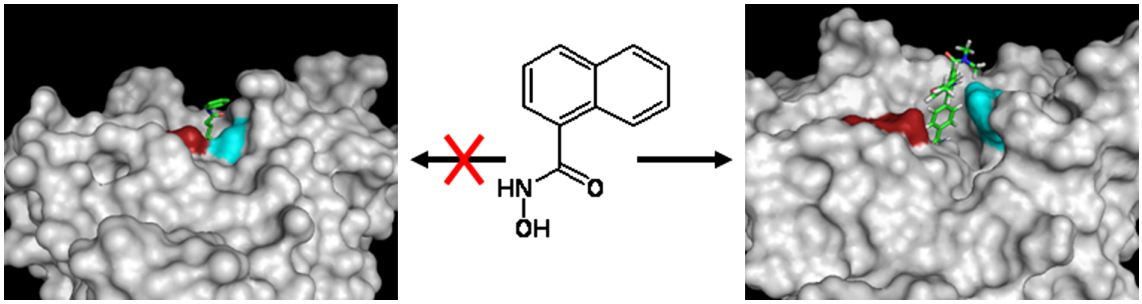

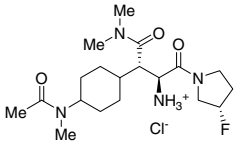

25 DPP-4 IC_{50} = 16 nM

A novel series of 4-aminophenylalanine and 4-aminocyclohexylalanine derivatives were designed and evaluated as inhibitors of dipeptidyl peptidase IV (DPP-4). The cyclohexylalanine derivatives such as **25** afforded PK exposure in rat and dog, and efficacy in a murine OGTT experiment.

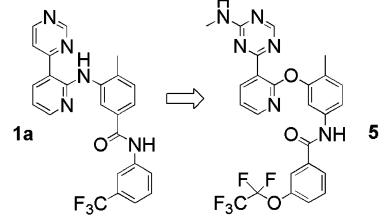

1a Tie-2: 4 nM, KDR: 4 nM → **5** Tie-2: 16 nM, KDR: 1,002 nM

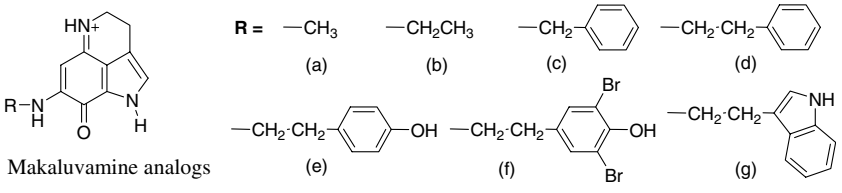

Makaluvamine analogs

Synthesis, topoisomerase II inhibition, and anticancer activities of makaluvamine analogs are presented.

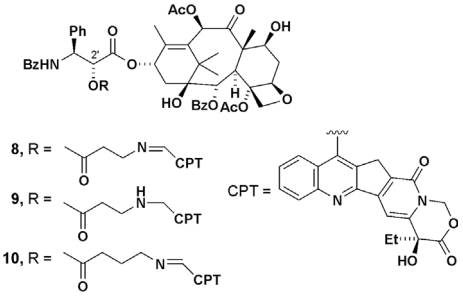

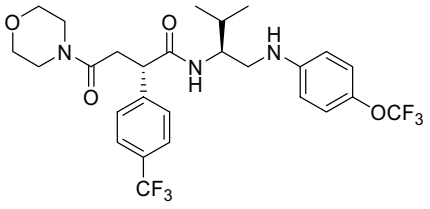

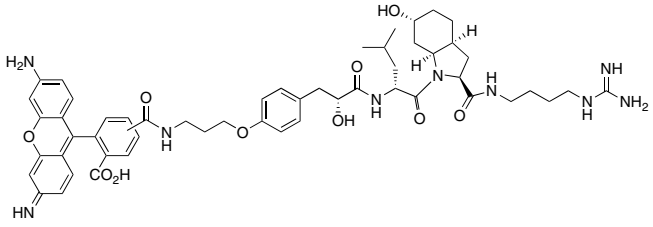

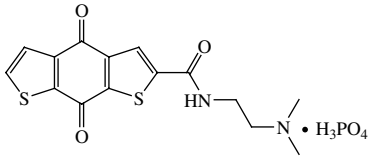

13

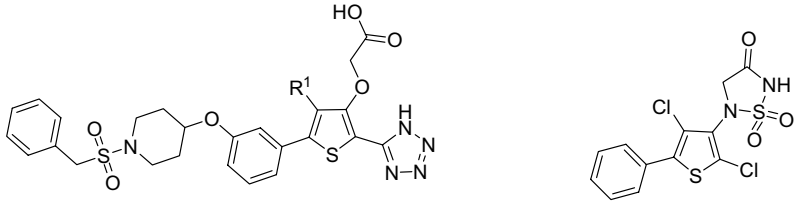

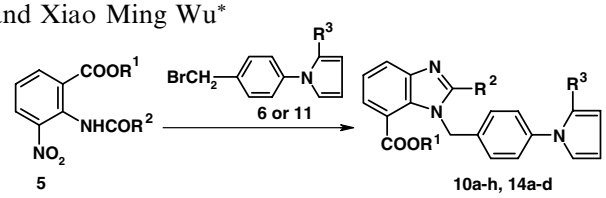

2-Alkylbenzimidazoles bearing a *N*-phenylpyrrole moiety **10a** and **10g** inhibited [^{125}I] AngII-binding affinity to AT_1 receptor at nanomolar level and evaluation in spontaneously hypertensive rats showed that **10a** is an orally active AT_1 receptor antagonist.

The synthetic entry to new classes of dual fXa/thrombin and selective thrombin inhibitors with significant oral bioavailability is described. The observed activity changes have been rationalised using structural studies.

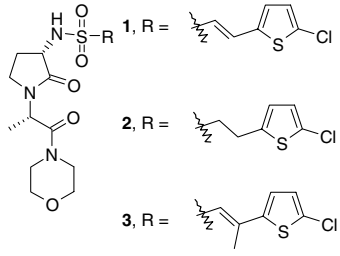

An example is presented where structural information combined with ab initio calculations clearly indicate that an observed difference in biological activity is dominated by sulfonamide-related conformational effects.

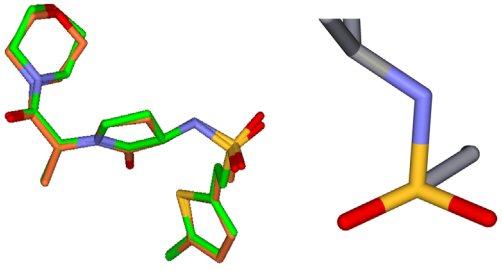

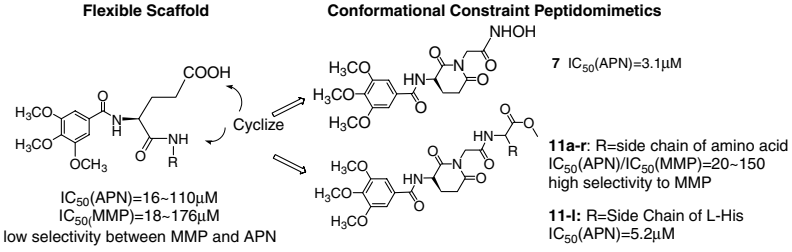

OTHER CONTENTS

*Corresponding author
ⓘ+ Supplementary data available via ScienceDirect

COVER

Typical snapshot of **7b** bound to HIV-RT from an MC simulation. Carbon atoms of **7b** are gold; from the left, Tyr181, Tyr188, Phe227, Leu100, Lys101; Trp229 at the top, Val106 at the bottom. H-bond with Lys101 O on right. Some residues in front including Glu138 have been removed for clarity. The water on N5 is also H-bonded to a carboxylate O of Glu138. [Thakur, V. T.; Kim, J. T.; Hamilton, A. D.; Bailey, C. M.; Domaoal, R. A.; Wang, L.; Anderson, K. S.; Jorgensen, W. L. *Bioorg. Med. Chem. Lett.* **2006**, *16*, 5664.]

Indexed/Abstracted in: Beilstein, Biochemistry & Biophysics Citation Index, CANCERLIT, Chemical Abstracts, Chemistry Citation Index, Current Awareness in Biological Sciences/BIOBASE, Current Contents: Life Sciences, EMBASE/Excerpta Medica, MEDLINE, PASCAL, Research Alert, Science Citation Index, SciSearch, TOXFILE

ELSEVIER

ISSN 0960-894X